D 3/5

A MODEL FOR PRESSURE IN AN LMFBR DUCT DUE TO DISCHARGE OF GAS FROM A FAILED FUEL PIN

S. SRINIVAS, P. S. CHOPRA

EBR-II Project, Argonne National Laboratory, 9700 South Cass Avenue, Argonne, Illinois 60439, U.S.A.

SUMMARY

In this paper an analytical model for the calculation of pressure pulses in hexagonal ducts due to discharge of gas from a failed fuel pin is developed. The analysis yields the time history of the pressure pulse which can be used in the calculation of permanent deformation of the duct or in the assessment of the susceptibility of the duct to fracture. The real physical situation of gas discharging through a pin in a duct filled with liquid is complex to model. Here the phenomenon is modeled based on some reasonable assumptions.

In this model the analysis is divided into two stages. In the first stage the gas expands as a spherical bubble, but the influence of the duct wall is taken into account. At the end of the first stage the spherical shape of the bubble is assumed to be lost and the gas is assumed to expand axially as a column. The analysis involves solving the continuity and momentum equations for the liquid along with the energy balance equation for the gas.

For stage 1 the continuity and momentum equations for the liquid in spherical coordinates are combined and integrated with respect to radius. This yields a differential equation in terms of the bubble radius, the bubble pressure, and the pressure at the effective radius of the duct. The liquid in the duct beyond the duct effective radius is assumed to flow axially, and is accelerated by the difference in pressure at the duct effective radius and the undisturbed pressure of the liquid. Based on this assumption an expression for pressure at the duct effective radius is obtained in terms of the bubble radius and its time derivatives.

The initial conditions for stage 1 are at time t_0, the bubble radius is equal to n times the duct effective radius and the bubble pressure is equal to the undisturbed liquid pressure. The time t_0 and the remaining initial conditions viz. bubble velocity are derived by using simplified forms of the governing differential equations for stage 1. The parameter n is obtained by matching the peak pressures obtained by present analysis with experimental results for a few cases. Its value was found to be 0.22.

For stage 2 the one-dimensional hydrodynamic equations are used. The initial conditions for stage 2 are the end conditions of stage 1. The stage 1 is ended after the bubble pressure becomes maximum or the bubble radius becomes equal to the duct effective radius, whichever occurs earlier.

Parametic studies of the bubble pressure and the pressure at the duct wall were conducted. The bubble pressure as well as pressure at the duct wall increase very rapidly with time, reach their maximum values, and then drop slowly. The peak bubble pressure as well as peak pressure at duct wall increase (1) as plenum pressure increases. (2) as area of duct decreases, and (3) as area of opening in the pin increases. The peak pressures increase slightly with increases in plenum volume and in duct length.

The pressure time history obtained by the present analysis can be used as input in STRAW or SADCAT codes to obtain permanent deformation of the duct.

1. Introduction

In this paper an analytical model for the calculation of the pressure pulse in hexagonal ducts due to discharge of gas from a failed fuel pin is developed. The analysis yields the time history of the pressure pulse which can be used in the calculation of permanent deformation of the ducts or in the assessment of the susceptibility of the duct to fracture.

In this model the analysis is divided into two stages: In the first stage the gas expands as a spherical bubble, but the influence of duct wall is taken into account. At the end of the first stage the spherical shape of the bubble is assumed to be lost and the gas is assumed to expand axially as a column. The end conditions of stage 1 are the initial conditions for stage 2. The analysis involves solving the continuity and momentum equations for the liquid along with the energy balance equation for the gas. In the analysis the liquid is assumed to be incompressible.

Chang et al., [1] and Kazimi [2] have developed models for calculation of the pressure pulse in hexagonal ducts due to discharge of gas from a failed fuel pin. Chang et al., assumed that the motion of the fluid is axial from the beginning. They also assumed a velocity distribution in the axial direction. Kazimi's model is similar to the first stage of expansion of the present model. Both Chang and Kazimi assume the initial conditions. In the present model the initial conditions are derived.

2. Nomenclature

A	=	area of opening in the failed fuel pin
A_f	=	final area of opening
A_h	=	effective cross-sectional area of the hexagonal duct
a	=	radius of the gas bubble in the first stage of expansion
B	=	plenum volume parameter = $V_p/\sqrt{RT_{p0}}$
b	=	$2s/3$
C	=	plenum pressure parameter = $P_{p0}\sqrt{RT_{p0}}$
C_d	=	coefficient of discharge
c_p, c_v	=	specific heats of gas
D	=	density of liquid
F	=	force due to impact of jet on the wall
g	=	acceleration due to gravity
H	=	$C_d \dfrac{(k-1)\sqrt{kg}}{2}\left(\dfrac{2}{k+1}\right)^{(k+1)/[2(k-1)]}$
h	=	half-length of gas column in the second stage of expansion
I	=	$1.5HC\,kA_f/[\pi(k-1)]$
k	=	ratio of specific heats of gas, c_p/c_v
L	=	half-length of duct
M_a	=	mass of gas in the bubble
M_p	=	mass of gas in the fuel pin
m	=	initial-velocity parameter
n	=	initial-bubble-radius parameter
P_a	=	gas-bubble pressure
P_0	=	undisturbed-liquid pressure

P_p	=	pressure of gas inside the fuel pin or plenum
P_{p0}	=	P_p at the beginning
P_s	=	liquid pressure at the duct wall
P_D	=	peak pressure at the duct wall
p	=	liquid pressure
q	=	velocity of discharging gas at the opening in the tube
R	=	gas constant
r	=	radius
S	=	$\int_0^t A\,dt$
s	=	effective radius of the duct $= \sqrt{A_h/\pi}$
T_a	=	gas-bubble temperature
T_p	=	temperature of gas inside the fuel pin or plenum
T_{p0}	=	T_p at the beginning
t	=	time
t_0	=	time at which initial conditions are obtained
U	=	axial velocity of liquid
u	=	radial velocity of liquid
V	=	gas-bubble volume
V_p	=	volume of gas in the fuel pin
w	=	rate of discharge of gas through opening
y	=	P_a/P_p for $P_a/P_p \geq y_c$; $=$ y_c for $P_a/P_p < y_c$
y_c	=	$[2/(k+1)]^{k/(k-1)}$

$\dot{}$ denotes differentiation with respect to time

3. Energy Balance Equation

The energy balance for the gas bubble is obtained by equating the enthalpy of the discharging gas to the increase in internal energy of the bubble plus the rate of work done due to expansion. Thus,

$$w\, c_p T_p = c_v \frac{d}{dt}(T_a M_a) + P_a \dot{V} \tag{1}$$

From the equation of state

$$M_a T_a = P_a V/R \tag{2}$$

Substituting eq. (2) in (1) and simplifying we obtain

$$\dot{P}_a = (wRT_p - P_a\dot{V})\, k/V \tag{3}$$

The rate of discharge of gas from the fuel pin is given by [3]

$$w = C_d A \left[\frac{2\,kg\,P_p^2}{RT_p\,(k-1)} \left(y^{\frac{2}{k}} - y^{\frac{k+1}{k}}\right)\right]^{1/2} \tag{4}$$

For the gas inside the fuel pin, assuming adiabatic expansion,

$$\frac{dM_p}{dt} = -w \tag{5}$$

$$T_p/T_{p0} = (P_p/P_{p0})^{(k-1)/k} \tag{6}$$

and

$$P_p V_p = M_p R T_p \tag{7}$$

Combining eqs. (4) - (7), we obtain

$$\frac{dP_p}{dt} = -\frac{C_d\, Ak}{B}\left[\frac{2kg}{(k-1)}\left(y^{\frac{2}{k}} - y^{\frac{k+1}{k}}\right)\right]^{1/2} P_{p0}^{\frac{1-k}{2k}}\, P_p^{\frac{3k-1}{2k}} \tag{8}$$

Equation (8) has to be solved along with other equations. Generally (as is found later), the bubble pressure is lower than the critical pressure, that is $y < y_c$. In such cases in eq. (8) y is replaced by y_c. After simplification eq. (8) becomes:

$$\frac{dP_p}{dt} = -\frac{2\ HkA}{B(k-1)}\, P_{p0}^{\frac{1-k}{2k}}\, P_p^{\frac{3k-1}{2k}} \tag{9}$$

Integration of eq. (9) from t = 0 to any time t yields:

$$P_p = P_{p0}/(1+HS/B)^{2k/(k-1)} \tag{10}$$

From eqs. (4), (6), and (10) we get:

$$wRT_p = \frac{2HC\ A}{(k-1)\quad (1+HS/B)^{(3k-1)/(k-1)}} \tag{11}$$

Substituting eq. (11) in (3)

$$\dot{P}_a = \left[\frac{2HC\ A}{(k-1)\quad (1+HS/B)^{(3k-1)/(k-1)}} - P_a\dot{V}\right] k/V \tag{12}$$

Equation (12) is valid for both stages of expansion. The volume of the gas bubble and, consequently, $\dot{V}$ are given by

$$\begin{aligned} &V = 4\pi a^3/3;\ \dot{V} = 4\pi a^2\dot{a} \text{ in first stage of expansion} \\ &V = 2hA_h;\ \dot{V} = 2\dot{h}A_h \text{ in second stage of expansion} \end{aligned} \tag{13}$$

We assume a constant area of opening from the beginning, i.e., $A = A_f$ and, consequently,

$$S = A_f t \tag{14}$$

4. Equations For The Liquid Region

4.1 First-Stage Expansion

As mentioned earlier in the first stage of expansion the gas is assumed to expand as a spherical bubble. The flow of liquid in the vicinity of the bubble is also assumed to be spherical and therefore the continuity equation for the liquid, assuming incompressibility is [4]

$$\frac{\partial}{\partial r}\,(r^2 u) = 0 \tag{15}$$

and the momentum equation is

$$D\,\frac{\partial u}{\partial t} + Du\,\frac{\partial u}{\partial r} + \frac{\partial p}{\partial r} = 0 \tag{16}$$

Integrating equation (15) with respect to r, we have

$$u = \dot{a}\, a^2/r^2 \tag{17}$$

Substituting eq. (17) in (16) and simplifying, we obtain

$$D\,\frac{a^2}{r^2}\,\ddot{a} + 2D\dot{a}^2\left(\frac{a}{r^2} - \frac{a^4}{r^5}\right) + \frac{\partial p}{\partial r} = 0 \tag{18}$$

Integrating eq. (18) with respect to r and using the boundary condition at a reference radius equal to the effective radius of the duct s, viz. at $r = s$, $p = P_s$, we have

$$p = P_s + Da^2\ddot{a}\left(\frac{1}{r} - \frac{1}{s}\right) + 2D\dot{a}^2\left(\frac{a}{r} - \frac{a}{s} - \frac{a^4}{4r^4} + \frac{a^4}{4s^4}\right) \tag{19}$$

At the liquid-bubble interface, i.e., $r = a$, $p = P_a$. Substituting this condition in eq. (19) we have

$$P_a = P_s + Da^2\ddot{a}\left(\frac{1}{a} - \frac{1}{s}\right) + 2D\dot{a}^2\left(\frac{3}{4} - \frac{a}{s} + \frac{a^4}{4s^4}\right) \tag{20}$$

We now derive an expression for P_s the pressure at the reference radius s, taking into account the effect of the duct wall. We assume that the liquid motion beyond radius s is axial and its velocity is uniform. From continuity considerations (assuming symmetry of flow about the midplane of the duct),

$$A_h U = \dot{V}/2 = 2\pi a^2\dot{a} \tag{21}$$

The difference in the pressure at radius s, P_s, and the pressure at the end of the duct, P_0, accelerates the liquid in the duct outside the radius s. The volume of liquid is equal to $LA_h - \frac{1}{2}\frac{4\pi s^3}{3} = A_h(L-b)$. Thus, from momentum considerations

$$\dot{U} = \frac{P_s - P_0}{D\,(L-b)} \tag{22}$$

Combining equations (21) and (22)

$$P_s = 2D(L-b)\;(2a\,\dot{a}^2 + a^2\ddot{a})/s^2 + P_0 \tag{23}$$

Substituting (23) in (20) and solving for $\ddot{a}$, we obtain

$$\ddot{a} = \left[\frac{P_a - P_0}{D} - \dot{a}^2\left(\frac{3}{2} - \frac{2a}{s} + \frac{a^4}{2s^4} + \frac{4a(L-b)}{s^2}\right)\right] \Big/ \left[a(1 - a/s) + 2a^2\,(L-b)/s^2\right] \tag{24}$$

Equations (12) and (24) are the governing equations for the first-stage expansion.

4.2 Initial Conditions

If we assume the initial conditions at $t = 0$, $\dot{a} = 0$ and $P_a = P_0$, the governing differential equations (12) and (21) are not numerically integrable. To circumvent this difficulty in reference [2] a non-zero value was assumed for a at $t = 0$. The results of the analysis are very sensitive to the choice of initial conditions. In contrast, we derive the initial conditions at a time t_0 which is very close to zero. At the beginning of expansion the effect of the duct wall will be negligible and, consequently, we substitute ∞ for s in eq. (24). This yields

$$\ddot{a} = \frac{P_a - P_0 - 1.5\,D\dot{a}^2}{Da} \tag{25}$$

Combining equations (12), (14) and (25) and neglecting the small order term (HS/B) we obtain the equation

$$Da^4\ddot{a} + D(4 + 3k)\ddot{a}\,\dot{a}\,a^3 + 4.5kDa^2\dot{a}^3 + 3kP_0\dot{a}a^2 - I = 0 \tag{26}$$

Integrating eq. (26) once with respect to t between the limits 0 and t_0, we obtain

$$Da_0^4\ddot{a}_0 + 1.5kDa_0^3\dot{a}_0^2 + kP_0a_0^3 - It_0 = 0 \tag{27}$$

where a_0, $\dot{a}_0$ and $\ddot{a}_0$ refer to the values of a, $\dot{a}$, and $\ddot{a}$ at $t = t_0$. Now we assume that the bubble pressure P_a remains equal to the undisturbed liquid pressure P_0 during this initial period. Therefore, from eq. (25)

$$a_0\ddot{a}_0 = -1.5\dot{a}_0^2 \tag{28}$$

We can also write

$$\dot{a}_0 = ma_0/t_0 \text{ and,} \tag{29}$$

$$a_0 = ns$$

where m and n are known constants. Substitution of eqs. (28) and (29) in (27) yields

$$It_0^3 - (kP_0 s^3 n^3)t_0^2 - 1.5(k-1)Dm^2 s^5 n^5 = 0 \tag{30}$$

Solving eq. (30) the only positive value of t_0 is obtained. Thus the initial conditions are at $t = t_0$, $a = ns$, $\dot{a} = \dot{a}_0$ (obtained from eq. (29)), and $P_a = P_0$. The values of m and n are chosen by matching analytical results with experimental values for peak pressures.

The pressure at the duct wall is obtained from eq. (23). The pressure in the liquid at any radius r is obtained using equation (19).

4.3 Second-Stage Expansion

In the second-stage expansion the bubble expansion and the flow of the liquid is assumed to be uniform and consequently the velocity of the liquid is equal to the rate of expansion of the bubble. Therefore, the velocity of the liquid U can be written in terms of half the length of the bubble h as

$$U = \frac{dh}{dt} \tag{31}$$

Equation (22), with b replaced by h and P_s replaced by P_a, is valid for the second-stage;

$$\dot{U} = \frac{P_a - P_0}{D(L-h)} \tag{32}$$

Equations (12), (31), and (32) are the governing equations for the second-stage of expansion. The bubble pressure, bubble volume and the liquid velocities at the beginning of the second stage are equal to the corresponding values at the end of first stage. The bubble length at the beginning of the second stage is obtained by dividing the bubble volume at the end of first stage by the cross-sectional area of the duct.

5. Results

The numerical integration of the simultaneous ordinary differential equations was conducted using the Runge-Kutta method. The first-stage expansion was terminated and the second-stage expansion was begun when the first-stage bubble pressure reached a maximum value or the bubble radius equaled the effective radius of the duct, whichever occurred first.

The time history of the pressure at the duct wall obtained in an experiment [5] in which the volume of Argon gas in the tube was 4.3 cc, initial temperature and pressures were 70°F (21°C) and 3100 psi (21.4 MPa), and area of opening was 0.047 in^2 (0.303 cm^2) is plotted in Fig. 2. The liquid in the duct was water at atmospheric pressure. The bubble pressure and the pressure at the duct wall predicted by the present analysis are also plotted for m = 0.1 and n = 0.216. The corresponding initial conditions were t_0 = 0.0138 msec, a_0 = 0.254 in (0.645 cm), $\dot{a}_0$ = 1850 in/sec (47 m/sec), and P_0 = 14.5 psi (0.1 MPa). The values of m and n were adjusted such that the predicted peak pressure agreed with experimental peak pressure. However, the predicted peak pressure occurrs before the experimental peak. This is probably because in the calculation instantaneous opening was assumed, but in practice the opening might be gradual, however fast it might be. It is seen from the figure that the pressure rises rapidly, reaches a maximum and then decreases slowly.

The effects of plenum pressure parameter, plenum volume parameter, duct length, area of cross-section of duct, undisturbed liquid pressure, liquid density, and area of opening in the fuel element are shown in Figs. 3 through 10 and are summarized in Table I. The variation in the ratio of specific heats of the gas within the range of 1.6 - 1.7 has insignificant influence on the duct pressure, and consequently the influence of the type of gas (Argon, Xenon, Krypton and Helium) is through its gas constant. Therefore, for a mixture of gases the effective gas constant is used in the analysis.

In Fig. 11 the values of peak duct pressure obtained from the present analysis are compared with the examples given in Ref. [1]. The analysis in Ref. [1] yields peak pressure which are much lower than those of present analysis. One of the reasons is the opening assumed in Ref. [1] is gradual, whereas in the present analysis we assume an instantaneous opening with an area equal to the final area. However, if we choose in the present analysis an area equal to that at the time when pressure reaches its peak in Ref. [1], peak pressure values obtained from present analysis and Ref. [1] are close.

6. Defective Fuel Pin Adjacent To Wall

When the defective fuel pin is at the center of the duct the expansion of the gas as well as the flow of the liquid will not be disturbed, because they are axisymmetric, by the placement of a rigid sheet whose vertical axis coincides with that of the duct. Therefore the expansion of the gas and the flow of the liquid in the case of a defective fuel pin adjacent to wall (Fig. 12) can be treated as approximately equivalent to that of a fuel pin at the center of the duct with an effective duct cross-sectional area and discharge rate equal to twice the actual values. In addition, in the case of the defective fuel pin adjacent to wall if the opening faces the wall there will be a force on the wall due to the impact of the jet of gas. The center of action of this force is opposite to the center of the opening in the tube, and the force is equal to the product of the discharge rate and the velocity of gas at the wall. Since the tube is very close to the wall, the velocity of gas at the wall can be assumed to be equal to the velocity of gas at the opening (q). Thus,

$$F = wq \tag{33}$$

The discharge rate w is given by eq. (4) and the velocity q is given by [3]

$$q = \left[\frac{2kRgT_p}{k-1}\left(1 - y^{(1-k)/k}\right)\right]^{1/2} \tag{34}$$

For the calculation of impact force the *actual* discharge rate is used.

7. Concluding Remarks

In this paper a simple model for obtaining the pressure on the duct wall due to discharge of fission gas from a fuel pin was developed. Plenum pressure, plenum temperature, type of gas, duct effective area of cross-section and area of opening were found to be important parameters. Plenum volume, length of duct, type of liquid, and undisturbed liquid pressure were found to have less influence on peak duct pressures. The pressure-time history obtained from this analysis can be used to obtain either the permanent deformation experienced by the duct [6] or to assess the susceptibility of the duct to fracture.

Table I. Influence of Various Parameters On Peak Duct Pressure, (P_D)

Parameter	Figure	Effect of Increase in the Value of the Parameters On Peak Duct Pressure, (P_D)	Remarks
Plenum pressure parameter (C)	3	Increases	P_D increases with plenum pressure
Plenum volume parameter (B)	4	Increases at lower values of B. For B > 5 the increase is slight (seems to approach an asympotic value)	P_D increases slightly with increase in plenum volume for B > 5. Therefore test results obtained for one value of B can be used for other values as long as B > 5 and other parameters are same.
Product of initial plenum temperature and gas constant (RT_{p0})	5	Increases slightly	Plenum temperature and gas constant occur together in parameters B and C. For a given plenum volume and initial plenum temperature and pressure, P_D increases with increase in R. Thus Xenon gives rise to lower P_D then Argon.
Duct Length (L)	6	Increases slightly (approaches an asymptotic value)	Test results obtained for shorter ducts can be used for longer ducts without significant errors.
Duct effective area of cross-section (A_h)	7	Decreases rapidly	Test results obtained without simulating the cluster of fuel pins cannot be used for ducts with cluster in them.
Undisturbed liquid pressure P_0	8	Increases slightly	Test results obtained at lower values of P_0 can be used for higher values of P_0 without significant errors.

Table I (Cont'd.)

Parameter	Figure	Effect of Increase in the Value of the Parameters On Peak Duct Pressure, (P_D)	Remarks
Density of the liquid	9	Increases slightly	Test results obtained with water can be used for sodium.
Area of opening in the fuel element	10	Increases	Area of opening is an important parameter.

References

[1] L. K. Chang, G. H. Golden, A. M. Judd and J. F. Koenig, "Pressure Pulse on a Sub-assembly Wall Due to Gas Release from A Failed Pin," Nuclear Engg. and Design, Vol. 31, 1974, pp. 72-76.

[2] M. S. Kazimi, "Analysis of Pressure Pulse Generation Due to Gas Release from Failed Fuel Pins in a LMFBR," Nuclear Science and Technology, Vol. 59, 1976, pp. 1-11.

[3] N. C. Ebaugh, Engineering Thermodynamics, Van Nostrand Co., Inc., New York, 1952.

[4] R. H. Cole, Underwater Explosions, Princeton University Press, Princeton, 1948.

[5] J. F. Koenig, C. C. Price, and D. H. Napper, Trans. Am. Nucl. Soc., Vol. 14, 1971, p. 286.

[6] P.S. Chopra and S. Srinivas, "On the Dynamic Response of EBR-II Ducts to Pressure Pulses," Nuclear Engg. & Design, Vol. 38, 1976, pp. 15-27.

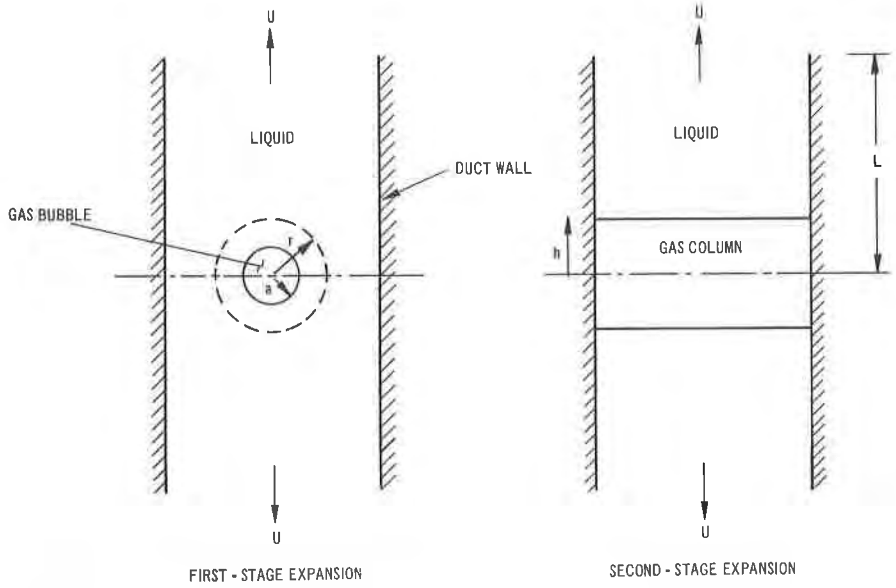

Fig. 1 : Bubble Configuration.

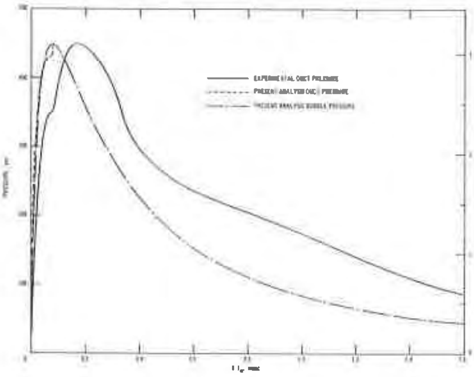

Fig. 2 : Pressure-Time History
P_{p0} = 3100 psi (21.4 MPa), V_p = 0.262 cm^3 (4.3 cc), T_{p0} = 70°F (21.1°C), Gas = Argon, A_f = 0.047 in^2 (0.303 cm^2), Liquid = water, P_0 = 14.5 psi (0.1 MPa), A_h = 4.2 in^2 (27.1 cm^2), L = 8 in (20.3 cm).

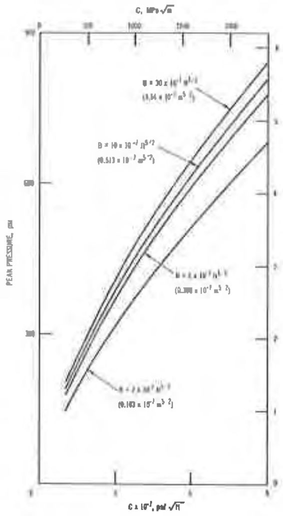

Fig. 3 :
Peak Duct Pressure vs Plenum Pressure Parameter
A_f = 0.0265 in^2 (0.171 cm^2), Liquid = water, P_0 = 14.5 psi (0.1 MPa), A_h = 1.89 in^2 (12.2 cm^2), L = 25 in (63.5 cm).

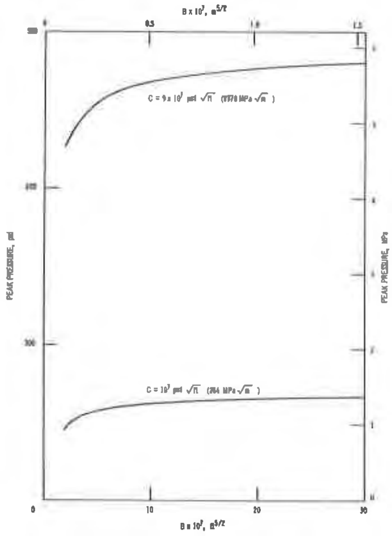

Fig. 4 :
Peak Duct Pressure vs Plenum Volume Parameter
A_f = 0.0265 in^2 (0.171 cm^2), Liquid = water, P_0 = 14.5 psi (0.1 MPa), A_h = 1.89 in^2 (12.2 cm^2), L = 25 in (63.5 cm).

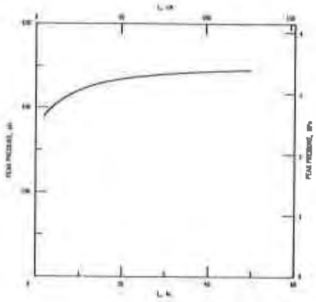

Fig. 6 :

Peak Duct Pressure vs Duct Length
P_{p0} = 2000 psi (13.8 MPa), V_p = 0.25 in^3 (4.1 cc), T_{p0} = 70°F (21.1°C), Gas = Argon, A_f = 0.0265 in^2 (0.171 cm^2), Liquid = water, P_0 =14.5 psi (0.1 MPa), A_h = 1.89 in^2 (12.2 cm^2).

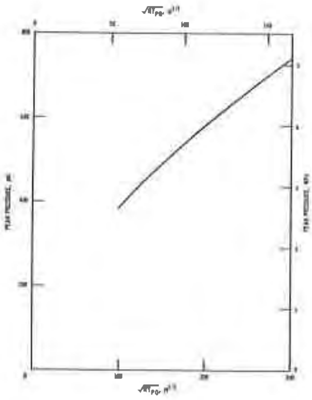

Fig. 5 :

Peak Duct Pressure vs Product of Initial Plenum Temperature and Gas Constant
P_{p0} = 2000 psi (13.8 MPa), V_p = 0.25 in^3 (4.1 cc), A_f = 0.0265 in^2 (0.171 cm^2), Liquid = water, P_0 = 14.5 psi (0.1 MPa), A_h = 1.89 in^2 (12.2 cm^2), L = 25 in (63.5 cm).

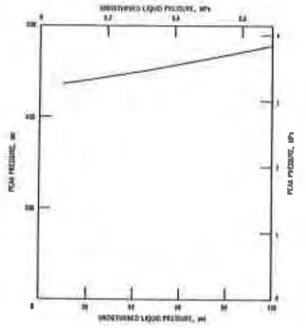

Fig. 8 :

Peak Duct Pressure vs Undisturbed Liquid Pressure
P_{p0} = 2000 psi (13.8 MPa), V_p = 0.25 in^3 (4.1 cc), T_{p0} = 70°F (21.1°C), Gas = Argon, A_f = 0.0265 in^2 (0.171 cm^2), Liquid = water, A_h = 1.89 in^2 (12.2 cm^2), L = 25 in (63.5 cm).

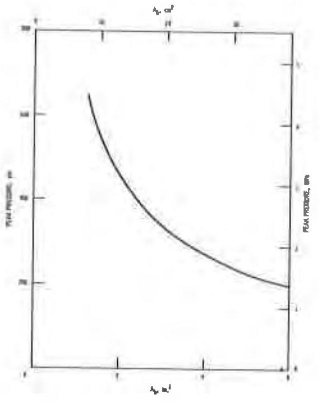

Fig. 7 :

Peak Duct Pressure vs Duct Effective Area of Cross-section
P_{p0} = 2000 psi (13.8 MPa), V_p = 0.25 in^3 (4.1 cc), T_{p0} = 70°F (21.1°C), Gas = Argon, A_f = 0.0265 in^2 (0.171 cm^2), Liquid = water, P_0 = 14.5 psi (0.1 MPa), L = 25 in (63.5 cm).

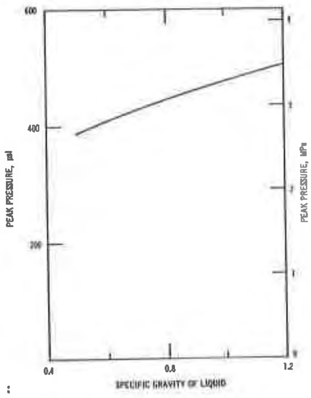

Fig. 9 :

Peak Duct Pressure vs Specific Gravity of the Liquid
P_{p0} = 2000 psi (13.8 MPa), V_p = 0.25 in^3 (4.1 cc), T_{p0} = 70°F (21.1°C), Gas = Argon, A_f = 0.0265 in^2 (0.171 cm^2), P_0 = 14.5 psi (0.1 MPa), A_h = 1.89 in^2 (12.2 cm^2), L = 25 in (63.5 cm).

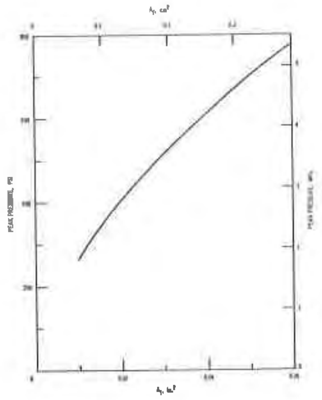

Fig. 10:

Peak Duct Pressure vs Area of Opening in the Fuel Pin
P_{p0} = 2000 psi (13.8 MPa), V_p = 0.25 in^3 (4.1 cc), T_{p0} = 70°F (21.1°C), Gas = Argon, Liquid = water, P_0 = 14.5 psi (0.1 MPa), A_h = 1.89 in^2 (12.2 cm^2), L = 25 in (63.5 cm).

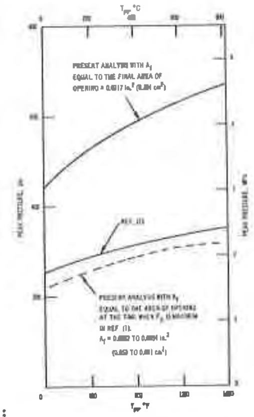

Fig. 11:

Peak Duct Pressure vs Initial Plenum Temperature
P_{p0} = 1500 psi (10.3 MPa), V_p = 0.49 in^3 (8 cc), Gas = Helium, Liquid = Sodium, P_0 = 14.5 psi (0.1 MPa), A_h = 3.84 in^2 (24.8 cm^2), L = 8.25 in (21 cm).

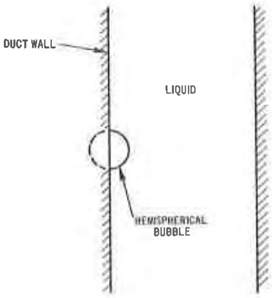

Fig. 12:

Bubble Configuration for Failed Fuel Pin Adjacent to Duct Wall.